

Autonomous zinc-finger nuclease pairs for targeted chromosomal deletion

Cem Şöllü^{1,2}, Kaweh Pars^{1,2}, Tatjana I. Cornu², Stacey Thibodeau-Beganny³, Morgan L. Maeder^{3,4}, J. Keith Joung^{3,4,5}, Regine Heilbronn² and Toni Cathomen^{1,2,*}

¹Department of Experimental Hematology, Hannover Medical School, Hannover, ²Institute of Virology, Campus Benjamin Franklin, Charité Medical School, Berlin, Germany, ³Molecular Pathology Unit, Center for Cancer Research, and Center for Computational and Integrative Biology, Massachusetts General Hospital, Charlestown, ⁴Biological and Biomedical Sciences Program and ⁵Department of Pathology, Harvard Medical School, Boston, MA, USA

Received May 25, 2010; Revised July 27, 2010; Accepted July 28, 2010

ABSTRACT

Zinc-finger nucleases (ZFNs) have been successfully used for rational genome engineering in a variety of cell types and organisms. ZFNs consist of a non-specific FokI endonuclease domain and a specific zinc-finger DNA-binding domain. Because the catalytic domain must dimerize to become active, two ZFN subunits are typically assembled at the cleavage site. The generation of obligate heterodimeric ZFNs was shown to significantly reduce ZFN-associated cytotoxicity in single-site genome editing strategies. To further expand the application range of ZFNs, we employed a combination of *in silico* protein modeling, *in vitro* cleavage assays, and *in vivo* recombination assays to identify autonomous ZFN pairs that lack cross-reactivity between each other. In the context of ZFNs designed to recognize two adjacent sites in the human HOXB13 locus, we demonstrate that two autonomous ZFN pairs can be directed simultaneously to two different sites to induce a chromosomal deletion in ~10% of alleles. Notably, the autonomous ZFN pair induced a targeted chromosomal deletion with the same efficacy as previously published obligate heterodimeric ZFNs but with significantly less toxicity. These results demonstrate that autonomous ZFNs will prove useful in targeted genome engineering approaches wherever an application requires the expression of two distinct ZFN pairs.

INTRODUCTION

Methods to introduce precise and stable modifications in complex genomes hold great potential not only for the study of gene function but also for biotechnological and therapeutical applications. A promising approach for rational genome engineering is based on the zinc-finger nuclease (ZFN) technology (1–3). ZFNs are artificial proteins that consist of a non-specific endonuclease domain, derived from the FokI restriction enzyme, and a specific DNA-binding domain, which consists of tandem repeats of engineered zinc-finger domains, each mediating binding to ~3 nt of DNA (4,5). Because the catalytic FokI domain has to dimerize to become active, two ZFN subunits are assembled at a cleavage site (6). Typically, a ZFN subunit contains three or four zinc-finger motifs that together recognize 9 or 12 bp, respectively. The combined target site is hence defined by a stretch of 18 or 24 bp, a sequence of sufficient length to be statistically unique in a complex genome.

Several reports have highlighted the power of ZFNs for studying biological systems in mammalian cells (7,8) or whole organisms, like the fruit fly (9), nematodes (10), zebrafish (11–13) or rats (14,15). Moreover, the high frequency of gene editing at endogenous loci in plant cells (16–19), in mammalian cells classically used for drug screening or protein production (20–22), or in primary human cells, including pluripotent stem cells (23–26), have demonstrated the wide application range of the ZFN technology in biology, biotechnology or human gene therapy.

Genome engineering by ZFNs is based on the enzyme's ability to activate the cellular DNA repair machinery by creating a DNA double-strand break in the target locus.

*To whom correspondence should be addressed. Tel: +49 511 532 5170; Fax: +49 511 532 5121; Email: cathomen.toni@mh-hannover.de
Present address

Tatjana I. Cornu, Epiontis GmbH, Berlin, Germany.

In the presence of an appropriately designed donor DNA, ZFNs are used to stimulate homologous recombination (HR) between the target locus and the donor DNA. In the absence of a donor DNA, cleavage by ZFNs is harnessed to disrupt a gene locus through the non-homologous end-joining (NHEJ) pathway (2,3). Very recently, the ability to create a targeted deletion in a chromosome by simultaneous expression of two ZFN pairs has been reported (21,27).

Despite these successes, ZFN-induced toxicity by cleavage at off-target sites has remained an important issue (27–29). ZFN variants that combine high activity with reduced toxicity have been generated by improving the DNA-binding specificities of the zinc-finger domains (16,30), by customizing the interdomain linkers (31,32), and/or by regulating the DNA-cleavage activity through re-design of the FokI protein–protein interface (33,34). In the latter case, the ZFN dimer interface was altered such that only heterodimeric ZFNs could form upon binding to DNA. Here, we extend this approach and report the identification and characterization of ZFN variants that permit the simultaneous expression of two pairs of obligate heterodimers, whose monomeric ZFNs do not cross-react with each other. This technological advancement is relevant for rational genome engineering approaches that are based on the concomitant expression of two ZFN pairs, such as targeted chromosomal deletions or editing the genome at two sites in parallel. We demonstrate that the combined expression of two autonomous ZFN pairs was as effective at inducing a chromosomal deletion as previously described obligate heterodimeric ZFNs but that preventing cross-reaction between the individual ZFN subunits reduced toxicity significantly.

MATERIALS AND METHODS

In silico analysis

Protein modeling of the FokI cleavage domain was done with DeepView v4.0 (<http://www.expasy.org/spdbv/>) (34,35). Energy calculations of the FokI dimers were performed using FoldX version 3.0beta (<http://foldx.org/references.jsp>). The energy function includes terms that have been found to be important for protein stability, including Van-der-Waals forces, intra- and intermolecular hydrogen-bond formation, electrostatic contributions of charged groups, solvation energy and salt concentration. Details are described elsewhere (34,36,37).

Plasmids

The zinc-finger DNA-binding domains contained in our ZFN expression plasmids were described previously (16,30,38). Vectors encoding ZFNs EB2-N and BA1-N, donor plasmid pUC.Zgfp, target plasmids pCMV.LacZsXX δ GFP (XX referring to the respective binding sites for BA1-N and/or EB2-N) have been described earlier (30,39). Lentiviral vector plasmid pLV-CMV.LacZsEBBA δ GFPiNwpre was generated by replacing the '3/1' target site in pLV-CMV.LacZs31 δ GFPiNwpre (40) by the 'EB/BA' target site 5'- tCACTGCGGCattaatGCAGAAGCCg (capital

letters indicated binding sites for EB2-N and BA1-N, respectively). The ZFN expression cassettes for the HOXB13-specific ZFNs were generated by releasing the zinc-finger domains from the OPEN selection plasmids (16) with XbaI/BamHI and then ligating them into the '2-in-1' plasmid in either the first position with NheI/BglIII or the second position with XbaI/BamHI. The '2-in-1' ZFN cassette is under control of a CMV promoter, and each ZFN contains a triple FLAG tag. The ZFN subunits are separated by a sequence encoding the T2A autoprotease (Figure 4b for more details). Mutations in the FokI domain were introduced using site-directed mutagenesis. The relevant sequences are indicated in Figures 1a, 3a and Supplementary Figure S2.

In vitro cleavage assay

ZFNs were expressed *in vitro* using the TNT SP6 Quick Coupled Transcription/Translation System according to the manufacturer's instructions (Promega). To verify equal expression levels, ZFNs were initially synthesized in the presence of L-[³⁵S]-methionine, separated by SDS-PAGE, and detected by autoradiography. The target DNA fragment was generated by PCR with *Pfu* polymerase (Stratagene) using plasmids pCMV.LacZsXX δ GFP as templates and primers 5'-tgcaccgctggataacgacat and 5'-gaacttcagggtcagcttgc (Eurofins MWG Operon) to amplify a 980-bp fragment. A target site for the restriction enzyme AgeI was located next to the ZFN target site and used as a positive control. For *in vitro* cleavage, 1 μ l of each TNT lysate containing one ZFN subunit was mixed with 200 ng of the DNA template, 1 μ g of BSA and NEBuffer 4 (50 mM potassium acetate, 20 mM Tris-acetate pH 7.9, 10 mM magnesium acetate, 1 mM dithiothreitol; New England Biolabs) in a total volume of 10 μ l. Where indicated, 100 mM NaCl was added to the reaction. After incubation at 37°C for 90 min the reaction was analyzed on a 1.2% agarose gel.

Quantitative cell-based recombination and toxicity assays

Human HEK293T cells and the HEK293-based target cell line 293EBBA were grown in DMEM (Gibco/Invitrogen) supplemented with 10% fetal calf serum (Gibco/Invitrogen). The polyclonal target cell line 293EBBA was generated by lentiviral transduction as previously described (40). To ensure that cells carry a single copy target, transduction was performed with an MOI <0.1. The quantitative chromosomal recombination and toxicity assays were performed as previously described (40). Briefly, cell line 293EBBA contains an integrated mutated EGFP target locus (δ EGFP) with an adjacent heterodimeric target site for ZFN subunits EB2-N and BA1-N (EB/BA). Five days after transfection with the ZFN expression vectors, a donor plasmid to rescue EGFP expression by HR and a DsRed-Express (REx) expression vector, the percentage of green and red cells was determined by flow cytometry. The percentage of green cells at Day 5 specifies the frequency of HR, while the relative decline in the number of red cells from Day 2 to Day 5 is a marker of ZFN-induced cytotoxicity. The extent of gene targeting is indicated as percentage of

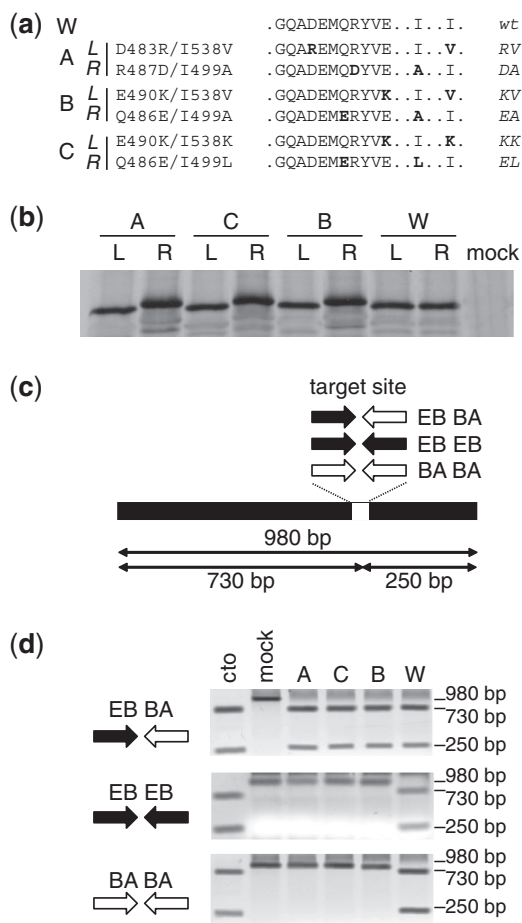


Figure 1. *In vitro* cleavage assay with obligate heterodimeric ZFNs. (a) Sequence of the *FokI* variants. The sequence is indicated for *FokI* positions 480–490 (helix $\alpha 4$), 499 and 538, and is shown for wild-type (W) and variants (A, B, C). The two-letter code on the right defines the corresponding point mutations in each subunit. (b) *In vitro* translated ZFNs. ZFNs were expressed in the presence of ^{35}S -met, separated by SDS-PAGE and exposed to X-ray film. L, left ZFN subunit EB2-N; R, right ZFN subunit BA1-N. (c) Schematic representation of *in vitro* cleavage assay. A linear DNA substrate containing the combined target site for ZFN subunits EB2-N and BA1-N (EB/BA) or inverted repeat target sites for subunits EB2-N (EB/EB) or BA1-N (BA/BA), respectively, are cleaved into different size products. (d) Analysis of heterodimeric or homodimeric cleavage reactions. A linear DNA substrate was incubated with *in vitro* translated ZFNs and the extent of cleavage analyzed by agarose gel electrophoresis. Control reactions were incubations with *in vitro* translated EGFP (mock) or *AgeI* (cto).

EGFP-positive cells normalized for transfection efficiency. The cell survival frequency is indicated as the fraction of REX-positive cells at day five as compared to Day 2 after transfection, normalized to a control transfection with a mutated nuclease.

Immunoblotting

Immunoblotting was basically performed as previously described (32). ZFNs were detected with antibodies directed against the HA tag (NB600-363; Novus Biologicals) or the FLAG tag (DYKDDDK tag antibody, Cell Signaling Technology), co-expressed

EGFP with antibody MAB3580 (Millipore). Proteins were visualized by infrared imaging after incubation with secondary antibodies conjugated with either IR-Dyes 680 or 800CW (LI-COR Biosciences).

Genotyping by PCR

200 000 HEK293T or 100 000 HeLa cells were seeded in 6-well plates 18 h before polyethyleneimine (PEI)-mediated transfection. The transfection mix contained 1.6 μg of each HOXB13-specific ZFN expression plasmid, 0.1 μg of pEGFP (Clontech) and pUC118 to 5 μg in PEI (0.1 g/l, pH 5.5) and 150 mM NaCl. Typically, >80% of cells were transfected as judged by flow cytometric measurement of EGFP-positive cells. Genomic DNA from transfected cells was extracted with the Blood MiniKit (Qiagen) and subsequent PCR analysis was performed with Phusion High-Fidelity DNA Polymerase (Finnzymes) in HF buffer using primers 5'-ggatggagccaaggatatcgaag and 5'-actgtccacaggcaacagg gagt (Eurofins MWG Operon). The PCR products were separated on a 1.2% agarose gel and quantified from non-saturated gel images with Quantity One V.4.6.5 software (Biorad).

Statistical analysis

All experiments were performed at least four times. Error bars represent standard deviation and statistical significance was determined using a one-sided, unpaired Student's *t*-test with unequal variance.

RESULTS

In vitro characterization of obligate heterodimeric ZFNs

An in-depth analysis of enzymatic reactions often requires the cumbersome production and purification of the individual components. Here, we used a simple *in vitro* transcription/translation system to generate small amounts of the nucleases for further *in vitro* characterization. Previously published ZFN dimerization variants (Figure 1a, Supplementary Figure S1); (33,34) were fused to well-characterized zinc-finger DNA-binding domains, termed BA1 and EB2 (30), synthesized *in vitro* (Figure 1b), and incubated with a PCR generated target DNA to assess their cleavage activity (Figure 1c). When using a DNA fragment with a target site for both subunits, the variant ZFN pairs displayed a similar cleavage activity as ZFNs with the wild-type *FokI* domain (Figure 1d, top panel). However, as opposed to the wild-type ZFN pair, none of the variant pairs was able to cleave DNA fragments with an inverted repeat target, i.e. where one subunit has to bind as a homodimer (Figure 1d, lower panels). This confirms that these three variant ZFNs act as true obligate heterodimers *in vitro*.

Identification of autonomous ZFN pairs

In order to identify obligate heterodimeric ZFN pairs that do not cross-react with each other, we performed extensive *in silico* analysis. DeepView was used to generate structural models of the various combinations of the *FokI*

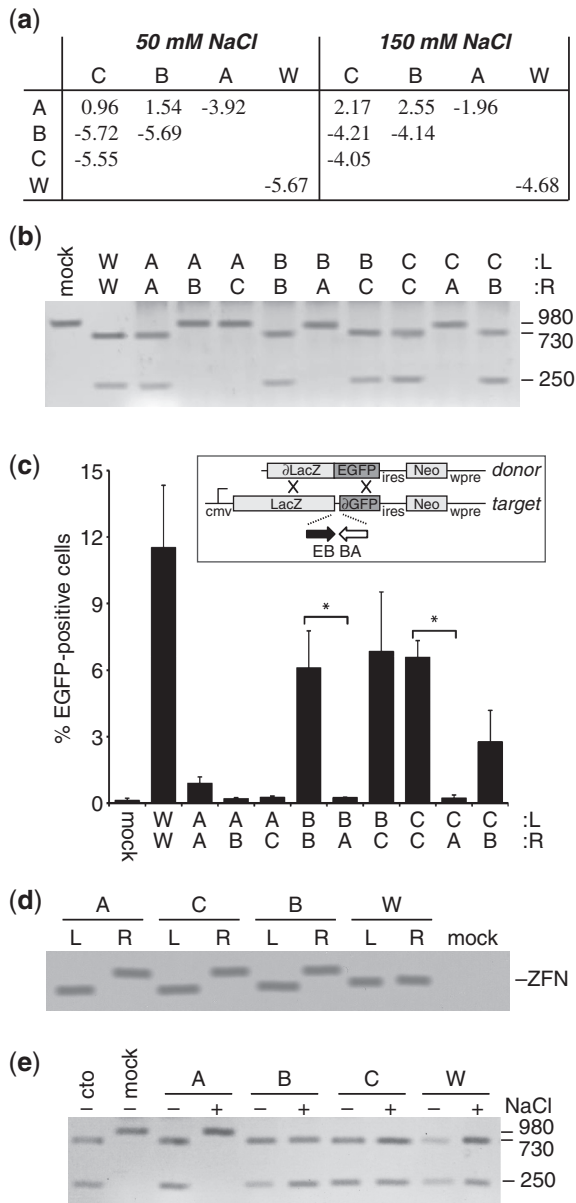


Figure 2. Comprehensive analysis of obligate heterodimeric ZFNs. **(a)** *In silico* computation of dimerization energy. The interaction energy of two variant ZFN subunits was calculated using FoldX based on structural models created with DeepView. The table indicates the average of the two calculated values (in kJ/mol) obtained when computing left-right versus right-left. **(b)** *In vitro* cleavage assay. A linear DNA substrate containing the heterodimeric target site for subunits EB2-N (L) and BA1-N (R) was incubated with *in vitro* translated ZFN variants in different combinations and the extent of cleavage analyzed by agarose gel electrophoresis. Control reactions were incubations with *in vitro* translated EGFP (mock) or wild-type ZFN (W). **(c)** Chromosomal recombination assay. Cell line 293EBBA contains an integrated mutated EGFP target locus (Δ EGFP) with an adjacent heterodimeric target site for ZFN subunits EB2-N and BA1-N (EB/BA). After transfection with the various ZFN expression vectors and a donor plasmid, the percentage of EGFP-positive cells was assessed by flow cytometry. An expression vector encoding a mutated nuclease (mock) was included as a control to indicate the level of non-stimulated gene targeting. A statistically significant ($P < 0.005$) decrease in gene targeting between homologous and heterologous ZFN subunit combinations is indicated by asterisks. **(d)** ZFN expression levels. Transfected HEK293T cells were harvested after 30 h and lysates probed with an antibody against the HA tag. 'mock' indicates transfection with an EGFP-expression vector. **(e)** Sensitivity to high

cleavage domain followed by calculation of the respective dimerization energies by FoldX at two different salt concentrations (Figure 2a). The *in silico* analysis predicted that 'opposite' ZFN pairs consisting of subunits that harbor FokI variants from pairs B and C should be active (dimerization energies similar to the wild-type configuration), while any combination between ZFN subunits from pairs A and B or pairs A and C, respectively, are not (positive dimerization energy). As shown in Figure 2b, these predictions could be verified using the *in vitro* cleavage assay. It is not surprising that ZFN combinations between variants from pairs B and C were still active because the respective FokI domains vary at only one amino acid position (Figure 1a). However, any combination of ZFN subunits from pairs A and B or pairs A and C, respectively, did not cleave the DNA target. The same ZFN combinations were tested further in a previously described cellular recombination assay (30,34), which is based on the rescue of a mutant EGFP gene. As ZFN-mediated cleavage of the chromosomally integrated, mutated reporter gene stimulates HR with a corrective donor DNA, the percentage of EGFP-positive cells reflects the activity of the respective ZFN combinations (Figure 2c). Transfection of the human HEK293-based reporter cell line with expression plasmids for ZFN variant pairs B/B and C/C revealed a decrease in the percentage of EGFP-positive cells as compared to wild-type ZFN, suggesting some attenuation due to the altered dimer interface. As seen *in vitro*, ZFN pairs B/C and C/B interacted with each other and supported correction of the mutant EGFP gene. Transfection of any combination of ZFN subunits from pairs A and B or pairs A and C, respectively, showed no substantial activity. However, ZFN pair A/A revealed only little activity compared to wild-type, suggesting that this variant is strongly attenuated. This significant drop in activity is likely a function of the considerable increase in the dimerization energy (Figure 2a) and not of the protein-expression level (Figure 2d). To further test this hypothesis, we repeated the *in vitro* cleavage assay using a higher salt concentration (Figure 2e). When adding 100 mM NaCl to the reaction, ZFN variant A/A was not able to cleave the DNA, substantiating that the lower cleavage activity is due to highly attenuated dimerization.

The FokI single amino acid exchange variant pair D483R/R487D is similar to pair A but lacks the additional mutations that destabilize the hydrophobic interaction (Figure 3a). We and others have previously shown that D483R/R487D, here termed pair 0, is an obligate heterodimer (8,12,33,34). *In silico* examination predicted that ZFN pair 0 should be more active than pair A and that the '0' subunits should not interact with ZFN subunits from pairs B and C (Figure 3b). These

salt concentrations. The linear DNA target was incubated with the *in vitro* translated variant ZFN pairs and the extent of cleavage analyzed by agarose gel electrophoresis. (+) or (-) indicates the presence or absence of an additional 100 mM NaCl in the reaction. Control reactions were incubations with *in vitro* translated EGFP (mock) or AgeI (cto). A, B, C, and W denote FokI variants as defined in Figure 1a.

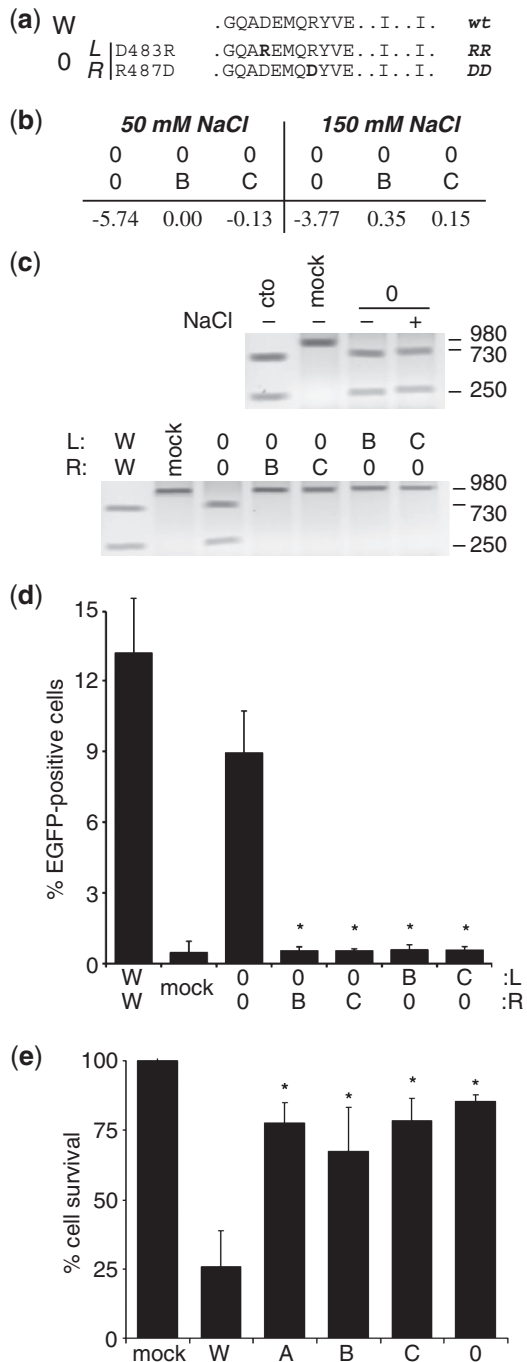


Figure 3. Identification of autonomous ZFN variants. (a) Sequence of the FokI variant pair 0. The sequence is indicated for FokI positions 480–490 (helix α 4), 499 and 538. The two-letter code on the right defines the corresponding point mutation in each subunit. (b) *In silico* computation of dimerization energy. The table indicates the average of the two calculated values (in kJ/mol) obtained when computing left–right versus right–left. (c) *In vitro* cleavage assays. A linear DNA substrate was incubated with *in vitro* translated ZFNs and the extent of cleavage analyzed by agarose gel electrophoresis. Top: the linear DNA target was incubated with variant ZFN pair 0. (+) or (–) indicates the presence or absence of an additional 100 mM NaCl in the reaction. Bottom: subunits of variant 0 were combined with the respective subunits of variants B and C. Control reactions were incubations with *in vitro* translated EGFP (mock), wild-type ZFN (W) or AgeI (cto). (d) Chromosomal recombination assay. Target cell line 293EBBA was transfected as in (Figure 2c) with combinations of the various ZFN expression vectors. The columns designate the percentage

predictions were verified by *in vitro* cleavage assays. ZFN pair 0 was active under high salt concentrations (Figure 3c, upper panel) and the respective subunits did not form active ZFNs when combined with the subunits of pairs B and C (Figure 3c, lower panel). These observations were confirmed in the cellular EGFP rescue assay, which indicated that none of the tested combinations, except pair 0/0, stimulated HR (Figure 3d). A comparison with combinations B/B and C/C revealed that ZFN variant 0/0 showed similar activity in HEK293 cells (compare to Figure 2c). To evaluate the ZFN-associated toxicity of these variants, cells were transfected with high amounts of the corresponding ZFN expression plasmids and spiked with an EGFP vector. Relative survival of cells, as determined by flow cytometry in comparison to cells transfected with a control expression plasmid, revealed that all obligate heterodimeric ZFN variants induced significantly less cytotoxicity than wild-type ZFN (Figure 3e). Together, this panel of *in silico*, *in vitro* and *in cellula* results indicates that all variant ZFN pairs—with the exception of variant A—combine high activity with a significantly lower ZFN-associated toxicity. Moreover, these data suggest that ZFN variant 0 does not cross-react with variant pairs B and C.

Application of autonomously functioning ZFN pairs to targeted chromosomal deletion

In order to demonstrate that autonomously dimeric ZFN pairs have an advantage over cross-reacting pairs, we evaluated these variants for their use in creating a targeted chromosomal deletion in human cells. To this end, different combinations of variant FokI domains were fused to zinc-finger DNA-binding domains that target two sites in exon 1 of the human HOXB13 locus (16; Figure 4a and b, Supplementary Figure S2a). Immunoblotting revealed that the steady state levels of all ZFN constructs were similar (Figure 4c). Two days after transfecting HEK293T or HeLa cells with different combinations of these variant ZFNs, genomic DNA was extracted and exon 1 amplified by PCR (Figure 4d, Supplementary Figure S2b). The percentage of alleles that revealed deletions was ~10% for both cross-reacting (combination hx1/hx2 or hx6/hx7) and autonomous ZFN variants (combination hx1/hx3 or hx6/hx3) in either cell line. Clonal analysis of HEK293T cells transfected with hx1/hx3 followed by PCR-based genotyping revealed that 9 out of 59 analyzed clones harbored a deleted allele (Supplementary Figure S2c), thus verifying the

of EGFP-positive cells 5 days after transfection, as determined by flow cytometry. An expression vector encoding a mutated nuclease (mock) was included as a negative control. A statistically significant ($P < 0.002$) decrease in gene targeting between homologous and heterologous ZFN subunit combinations is indicated by asterisks. (e) Quantitative cytotoxicity assay. HEK293 cells were transfected as described in (d). The columns represent the fraction of DsRed-Express-positive cells at day 5 as compared to the fraction at Day 2 after transfection, and are shown relative to transfection with an expression vector encoding a mutated nuclease (mock). A statistically significant increase in cell survival as compared to wild-type ZFN (W) is indicated by (* $P < 0.01$). A, B, C, 0 and W denote FokI variants.

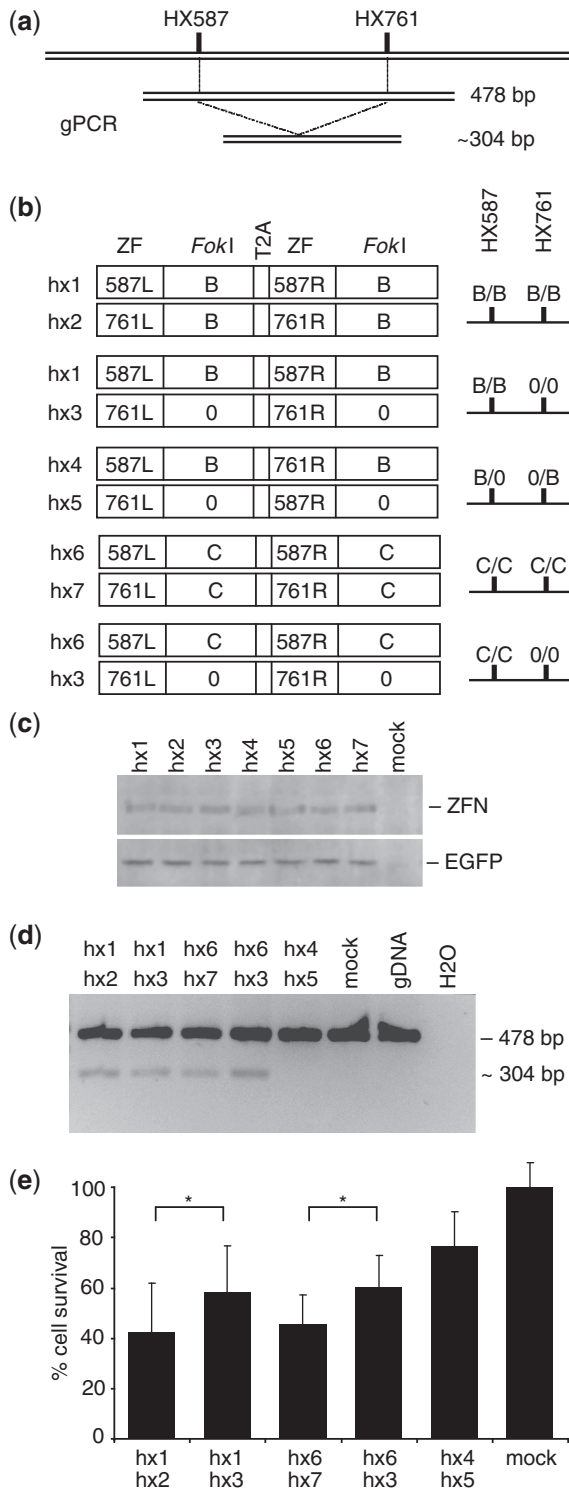


Figure 4. Targeted chromosomal deletion in human HOXB13 locus. **(a)** Diagram of genomic PCR strategy. ZFN target sites (HX587 and HX761) and possible PCR products are indicated. **(b)** Schematic representation of HOXB13-specific ZFN expression constructs. Each expression plasmid encodes two ZFN subunits, which are separated by a sequence encoding the T2A autoprotease. The plasmid names are shown on the left, the specificity of the DNA-binding domain and the respective FokI variant is indicated in the boxes. The FokI configuration of the five tested combinations at the two target sites is shown on the right. **(c)** ZFN expression levels. Lysates of HEK293T, which were co-transfected with ZFN expression vectors and pEGFP, were probed with antibodies against the FLAG tag and EGFP. Mock

calculated deletion frequency from Figure 4d. Importantly, expression of ZFN combination hx4/hx5 did not induce a detectable amount of chromosomal deletion. This demonstrates that the FokI variants 0 and B do not cross-react with each other although the zinc-finger domains mediate binding to the two target sites. Sequence analysis of HOXB13 alleles harboring the ZFN-induced deletion confirmed that the deletions are NHEJ-mediated fusions between the two ZFN half-sites at positions HX587 and HX761 (Supplementary Figure S2d). However, a cold shock—very recently shown to increase ZFN-mediated mutagenesis (41)—did not augment ZFN-mediated chromosomal deletion in either cell line (data not shown). Assessment of ZFN-associated cytotoxicity (Figure 4e) revealed that cell survival is significantly improved when comparing cross-reacting obligate heterodimeric ZFNs (hx1/hx2 or hx6/hx7, respectively) versus the autonomous ZFN pairs (hx1/hx3 or hx6/hx3, respectively). Taken together, these results show the advantage of employing autonomous ZFN pairs over cross-reacting ZFN pairs for the purpose of inducing a targeted chromosomal deletion in two different cell lines.

DISCUSSION

Toxicity upon expression of a single pair of ZFNs in human cells has been associated with off-target cleavage activity (8,23,28), the creation of unintentional chromosomal deletions (27), chromosomal instability at triplet repeats (42), and more generally, with apoptosis (39) and cell death (16,30,32–34,43). It seems therefore obvious that expression of two ZFN pairs in a single cell will further exacerbate these problems. If one were to use the wild-type FokI dimer interface on four ZFN monomers, this would lead to 12 possible dimeric permutations, which define 10 unique target sites. Even if one uses obligate heterodimeric FokI domains, four different pairs can form, all of which have the potential to induce DSBs at off-target loci. One potential solution to this problem is to generate ZFN pairs that do not cross-react with each other, so-called autonomous ZFN pairs. In this report, we describe the identification and characterization of two autonomous heterodimeric FokI domain pairs that we show can be utilized to induce a targeted chromosomal deletion. We demonstrate that the combined expression of two autonomous ZFN pairs that target adjacent sites in the human

indicates transfection with empty vectors. **(d)** Targeted chromosomal deletion. HEK293T were transfected with pEGFP and the indicated plasmids. PCR was performed on extracted genomic DNA and fragments separated by agarose gel electrophoresis. The size of the fragments is indicated on the right. Mock indicates transfection with a mutant nuclease and gDNA denotes a non-transfected control sample. **(e)** Quantitative cytotoxicity assay. HEK293T cells were transfected as described in (d). The columns represent the average fraction of EGFP-positive cells at Day 5 as compared to the fraction at Day 2 after transfection, and are shown relative to transfection with an expression vector encoding a mutated nuclease (mock). A statistically significant increase in cell survival between combinations hx1/hx2 and hx1/hx3 or hx6/hx7 and hx6/hx3 is indicated by (* $P < 0.05$). B, C and 0 denote FokI variants.

HOXB13 locus was as effective at inducing a chromosomal deletion as published obligate heterodimeric ZFN variants. Importantly, however, preventing cross-reaction between the individual ZFN subunits reduced toxicity significantly.

To identify pairs of autonomous ZFNs, we applied *in silico* protein modeling and energy calculations to characterize different combinations of variant FokI dimer interfaces. As reported previously (34), these computational analyses are a powerful tool to predict protein–protein interactions and, as established here, to predict the activity of ZFNs. The calculated energy threshold for efficient dimerization of ZFNs seems to be in the range of -2 kJ/mol. Any combination with a higher value turned out to be inactive in the *in vitro* cleavage assay or the cellular recombination assay. It should be noted that all variant FokI domains tested here showed a $\sim 30\%$ decrease in activity as compared to the wild-type configuration. However, the additional gain in specificity—as displayed e.g. by reduced toxicity—clearly outweighs this drop in activity.

We would like to point out a seeming discrepancy between the results obtained in this study and results published earlier (34), in which we reported that a ZFN with FokI variant A (RV/DA) worked more efficiently than ZFNs with variants B (KV/EA) or 0 (DD/RR). As recently reported (28), the zinc-finger DNA binding domains used in Szczepek *et al.* had a low specificity for their binding sites, as directly shown by their activity at off-target sites and indirectly demonstrated by the induction of massive cytotoxicity and apoptosis at even low ZFN concentrations (34,39). This is in agreement with the findings that the specificity of DNA-binding of a ZFN correlates with both its activity at the target site and reduced ZFN-associated toxicity (30). We believe that the high toxicity associated with the ZFN in Szczepek *et al.* obscured the readout for ZFN activity. A high nuclease activity (as in DD/RR) in combination with low DNA-binding specificity will induce massive cell death and therefore reduce the number of targeted cells in the population, while a ZFN variant with a highly attenuated nuclease activity (as in RV/DA) will induce less cytotoxicity and therefore seemingly increase the number of targeted cells. In conclusion, the actual contribution of the FokI domain to activity and toxicity of a ZFN can only be delineated when using zinc-finger domains with optimized DNA-binding parameters, such as zinc-finger arrays generated using the OPEN protocol (16).

In summary, autonomous ZFNs have a major advantage over simple obligate heterodimeric ZFNs, wherever an application requires the expression of two distinct ZFN pairs. It is safe to assume that the significant improvement in ZFN-associated toxicity, as measured in the transformed HEK293T cell line, is much more pronounced in sensitive primary cells and that the observed decrease in toxicity is based on reduced ZFN cleavage at off-target sites by preventing cross-reaction between the distinct ZFN pairs. Major applications of autonomous ZFN pairs will include the introduction of targeted chromosomal deletions (27) or forced translocations (44) to

answer biological questions. Founded on the improved safety profile, we also foresee applications in human gene therapy. For example, analogous to morpholino-induced therapeutic exon skipping for muscular dystrophy, ZFN-induced deletion of the mutation-containing exons could restore the open reading frame of dystrophin (45).

SUPPLEMENTARY DATA

Supplementary Data are available at NAR Online.

ACKNOWLEDGEMENTS

We thank Michal Szczepek for help with PyMOL 0.99rc6, Eva Guhl and Mathew Goodwin for technical assistance, Cherie Ramirez for constructing and providing the T2A ZFN expression cassette, François Stricher and Luis Serrano for advice on FoldX and Nadine Dannemann for critical reading of the article.

FUNDING

European Commission's 6th and 7th Framework Programmes (ZNIP-037783, PERSIST-222878 to T.C.); The National Institutes of Health (R01GM069906, R01GM088040, R21HL091808 to J.K.J.); fellowships from Charité Medical School (to C.S.); 'Kind-Philipp-Stiftung für Leukämieforschung' (to K.P.); the National Science Foundation (to M.L.M.), respectively. Funding for open access charge: European Commission's 7th Framework Programme, grant PERSIST-222878.

Conflict of interest statement. None declared.

REFERENCES

- Cathomen, T. and Schambach, A. (2010) Zinc positive: tailored genome engineering meets reprogramming. *Gene Ther.*, **17**, 1–3.
- Cathomen, T. and Joung, K.J. (2008) Zinc-finger nucleases: the next generation emerges. *Mol. Ther.*, **16**, 1200–1207.
- Carroll, D. (2008) Progress and prospects: zinc-finger nucleases as gene therapy agents. *Gene Ther.*, **15**, 1463–1468.
- Kim, Y.G., Cha, J. and Chandrasegaran, S. (1996) Hybrid restriction enzymes: zinc finger fusions to Fok I cleavage domain. *Proc. Natl Acad. Sci. USA*, **93**, 1156–1160.
- Rebar, E.J. and Pabo, C.O. (1994) Zinc finger phage: affinity selection of fingers with new DNA-binding specificities. *Science*, **263**, 671–673.
- Smith, J., Bibikova, M., Whitby, F.G., Reddy, A.R., Chandrasegaran, S. and Carroll, D. (2000) Requirements for double-strand cleavage by chimeric restriction enzymes with zinc finger DNA-recognition domains. *Nucleic Acids Res.*, **28**, 3361–3369.
- Urnov, F.D., Miller, J.C., Lee, Y.L., Beausejour, C.M., Rock, J.M., Augustus, S., Jamieson, A.C., Porteus, M.H., Gregory, P.D. and Holmes, M.C. (2005) Highly efficient endogenous human gene correction using designed zinc-finger nucleases. *Nature*, **435**, 646–651.
- Kim, H.J., Lee, H.J., Kim, H., Cho, S.W. and Kim, J.S. (2009) Targeted genome editing in human cells with zinc finger nucleases constructed via modular assembly. *Genome Res.*, **19**, 1279–1288.

9. Bibikova, M., Beumer, K., Trautman, J.K. and Carroll, D. (2003) Enhancing gene targeting with designed zinc finger nucleases. *Science*, **300**, 764.
10. Morton, J., Davis, M.W., Jorgensen, E.M. and Carroll, D. (2006) Induction and repair of zinc-finger nuclease-targeted double-strand breaks in *Caenorhabditis elegans* somatic cells. *Proc. Natl Acad. Sci. USA*, **103**, 16370–16375.
11. Doyon, Y., McCammon, J.M., Miller, J.C., Faraji, F., Ngo, C., Katibah, G.E., Amora, R., Hocking, T.D., Zhang, L., Rebar, E.J. et al. (2008) Heritable targeted gene disruption in zebrafish using designed zinc-finger nucleases. *Nat. Biotechnol.*, **26**, 702–708.
12. Meng, X., Noyes, M.B., Zhu, L.J., Lawson, N.D. and Wolfe, S.A. (2008) Targeted gene inactivation in zebrafish using engineered zinc-finger nucleases. *Nat. Biotechnol.*, **26**, 695–701.
13. Foley, J.E., Yeh, J.R., Maeder, M.L., Reyon, D., Sander, J.D., Peterson, R.T. and Joung, J.K. (2009) Rapid mutation of endogenous zebrafish genes using zinc finger nucleases made by Oligomerized Pool ENgineering (OPEN). *PLoS ONE*, **4**, e4348.
14. Mashimo, T., Takizawa, A., Voigt, B., Yoshimi, K., Hai, H., Kuramoto, T. and Serikawa, T. (2010) Generation of knockout rats with X-linked severe combined immunodeficiency (X-SCID) using zinc-finger nucleases. *PLoS ONE*, **5**, e8870.
15. Geurts, A.M., Cost, G.J., Freyvert, Y., Zeitler, B., Miller, J.C., Choi, V.M., Jenkins, S.S., Wood, A., Cui, X., Meng, X. et al. (2009) Knockout rats via embryo microinjection of zinc-finger nucleases. *Science*, **325**, 433.
16. Maeder, M.L., Thibodeau-Beganny, S., Osiaik, A., Wright, D.A., Anthony, R.M., Eichtinger, M., Jiang, T., Foley, J.E., Winfrey, R.J., Townsend, J.A. et al. (2008) Rapid “open-source” engineering of customized zinc-finger nucleases for highly efficient gene modification. *Mol. Cell*, **31**, 294–301.
17. Shukla, V.K., Doyon, Y., Miller, J.C., DeKolver, R.C., Moehle, E.A., Worden, S.E., Mitchell, J.C., Arnold, N.L., Gopalan, S., Meng, X. et al. (2009) Precise genome modification in the crop species *Zea mays* using zinc-finger nucleases. *Nature*, **459**, 437–441.
18. Townsend, J.A., Wright, D.A., Winfrey, R.J., Fu, F., Maeder, M.L., Joung, J.K. and Voytas, D.F. (2009) High-frequency modification of plant genes using engineered zinc-finger nucleases. *Nature*, **459**, 442–445.
19. Cai, C.Q., Doyon, Y., Ainley, W.M., Miller, J.C., DeKolver, R.C., Moehle, E.A., Rock, J.M., Lee, Y.L., Garrison, R., Schulenberg, L. et al. (2009) Targeted transgene integration in plant cells using designed zinc finger nucleases. *Plant Mol. Biol.*, **69**, 699–709.
20. Santiago, Y., Chan, E., Liu, P.Q., Orlando, S., Zhang, L., Urnov, F.D., Holmes, M.C., Guschin, D., Waite, A., Miller, J.C. et al. (2008) Targeted gene knockout in mammalian cells by using engineered zinc-finger nucleases. *Proc. Natl Acad. Sci. USA*, **105**, 5809–5814.
21. Liu, P.Q., Chan, E.M., Cost, G.J., Zhang, L., Wang, J., Miller, J.C., Guschin, D.Y., Reik, A., Holmes, M.C., Mott, J.E. et al. (2010) Generation of a triple-gene knockout mammalian cell line using engineered zinc-finger nucleases. *Biotechnol. Bioeng.*, **106**, 97–105.
22. Cost, G.J., Freyvert, Y., Vafiadis, A., Santiago, Y., Miller, J.C., Rebar, E., Collingwood, T.N., Snowden, A. and Gregory, P.D. (2010) BAK and BAX deletion using zinc-finger nucleases yields apoptosis-resistant CHO cells. *Biotechnol. Bioeng.*, **105**, 330–340.
23. Perez, E.E., Wang, J., Miller, J.C., Jouvenot, Y., Kim, K.A., Liu, O., Wang, N., Lee, G., Bartsevich, V.V., Lee, Y.L. et al. (2008) Establishment of HIV-1 resistance in CD4⁺ T cells by genome editing using zinc-finger nucleases. *Nat. Biotechnol.*, **26**, 808–816.
24. Zou, J., Maeder, M.L., Mali, P., Pruetz-Miller, S.M., Thibodeau-Beganny, S., Chou, B.K., Chen, G., Ye, Z., Park, I.H., Daley, G.Q. et al. (2009) Gene targeting of a disease-related gene in human induced pluripotent stem and embryonic stem cells. *Cell Stem Cell*, **5**, 97–110.
25. Hockemeyer, D., Soldner, F., Beard, C., Gao, Q., Mitalipova, M., DeKolver, R.C., Katibah, G.E., Amora, R., Boydston, E.A., Zeitler, B. et al. (2009) Efficient targeting of expressed and silent genes in human ESCs and iPSCs using zinc-finger nucleases. *Nat. Biotechnol.*, **27**, 851–857.
26. Lombardo, A., Genovese, P., Beausejour, C.M., Colleonis, S., Lee, Y.L., Kim, K.A., Ando, D., Urnov, F.D., Galli, C., Gregory, P.D. et al. (2007) Gene editing in human stem cells using zinc finger nucleases and integrase-defective lentiviral vector delivery. *Nat. Biotechnol.*, **25**, 1298–1306.
27. Lee, H.J., Kim, E. and Kim, J.S. (2010) Targeted chromosomal deletions in human cells using zinc finger nucleases. *Genome Res.*, **20**, 81–89.
28. Radecke, S., Radecke, F., Cathomen, T. and Schwarz, K. (2010) Zinc-finger nuclease-induced gene repair with oligodeoxynucleotides: wanted and unwanted target locus modifications. *Mol. Ther.*, **18**, 743–753.
29. Bohne, J. and Cathomen, T. (2008) Genotoxicity in gene therapy: an account of vector integration and designer nucleases. *Curr. Opin. Mol. Ther.*, **10**, 214–223.
30. Cornu, T.I., Thibodeau-Beganny, S., Guhl, E., Alwin, S., Eichtinger, M., Joung, J.K. and Cathomen, T. (2008) DNA-binding specificity is a major determinant of the activity and toxicity of zinc-finger nucleases. *Mol. Ther.*, **16**, 352–358.
31. Bibikova, M., Carroll, D., Segal, D.J., Trautman, J.K., Smith, J., Kim, Y.G. and Chandrasegaran, S. (2001) Stimulation of homologous recombination through targeted cleavage by chimeric nucleases. *Mol. Cell Biol.*, **21**, 289–297.
32. Händel, E.M., Alwin, S. and Cathomen, T. (2009) Expanding or restricting the target site repertoire of zinc-finger nucleases: the inter-domain linker as a major determinant of target site selectivity. *Mol. Ther.*, **17**, 104–111.
33. Miller, J.C., Holmes, M.C., Wang, J., Guschin, D.Y., Lee, Y.L., Rupniewski, I., Beausejour, C.M., Waite, A.J., Wang, N.S., Kim, K.A. et al. (2007) An improved zinc-finger nuclease architecture for highly specific genome editing. *Nat. Biotechnol.*, **25**, 778–785.
34. Szczepek, M., Brondani, V., Buchel, J., Serrano, L., Segal, D.J. and Cathomen, T. (2007) Structure-based redesign of the dimerization interface reduces the toxicity of zinc-finger nucleases. *Nat. Biotechnol.*, **25**, 786–793.
35. Guex, N. and Peitsch, M.C. (1997) SWISS-MODEL and the Swiss-PdbViewer: an environment for comparative protein modeling. *Electrophoresis*, **18**, 2714–2723.
36. Schymkowitz, J.W., Rousseau, F., Martins, I.C., Ferkinghoff-Borg, J., Stricher, F. and Serrano, L. (2005) Prediction of water and metal binding sites and their affinities by using the Fold-X force field. *Proc. Natl Acad. Sci. USA*, **102**, 10147–10152.
37. Schymkowitz, J., Borg, J., Stricher, F., Nys, R., Rousseau, F. and Serrano, L. (2005) The FoldX web server: an online force field. *Nucleic Acids Res.*, **33**, W382–W388.
38. Hurt, J.A., Thibodeau, S.A., Hirsh, A.S., Pabo, C.O. and Joung, J.K. (2003) Highly specific zinc finger proteins obtained by directed domain shuffling and cell-based selection. *Proc. Natl Acad. Sci. USA*, **100**, 12271–12276.
39. Alwin, S., Gere, M.B., Guhl, E., Effertz, K., Barbas, C.F. III, Segal, D.J., Weitzman, M.D. and Cathomen, T. (2005) Custom zinc-finger nucleases for use in human cells. *Mol. Ther.*, **12**, 610–617.
40. Cornu, T.I. and Cathomen, T. (2007) Targeted Genome Modifications Using Integrase-deficient Lentiviral Vectors. *Mol. Ther.*, **15**, 2107–2113.
41. Doyon, Y., Choi, V.M., Xia, D.F., Vo, T.D., Gregory, P.D. and Holmes, M.C. (2010) Transient cold shock enhances zinc-finger nuclease-mediated gene disruption. *Nat. Methods*, **7**, 459–460.
42. Mittelman, D., Moye, C., Morton, J., Sykoudis, K., Lin, Y., Carroll, D. and Wilson, J.H. (2009) Zinc-finger directed double-strand breaks within CAG repeat tracts promote repeat instability in human cells. *Proc. Natl Acad. Sci. USA*, **106**, 9607–9612.
43. Pruetz-Miller, S.M., Reading, D.W., Porter, S.N. and Porteus, M.H. (2009) Attenuation of zinc finger nuclease toxicity by small-molecule regulation of protein levels. *PLoS Genet.*, **5**, e1000376.
44. Brunet, E., Simsek, D., Tomishima, M., DeKolver, R., Choi, V.M., Gregory, P., Urnov, F., Weinstock, D.M. and Jasin, M. (2009) Chromosomal translocations induced at specified loci in human stem cells. *Proc. Natl Acad. Sci. USA*, **106**, 10620–10625.
45. Trollet, C., Athanasopoulos, T., Popplewell, L., Malerba, A. and Dickson, G. (2009) Gene therapy for muscular dystrophy: current progress and future prospects. *Expert Opin. Biol. Ther.*, **9**, 849–866.